



PCCP

OH radical reactions with the hydrophilic component of sphingolipids

Journal:	<i>Physical Chemistry Chemical Physics</i>
Manuscript ID	CP-ART-11-2020-005972.R1
Article Type:	Paper
Date Submitted by the Author:	22-Dec-2020
Complete List of Authors:	Lisovskaya, Alexandra; University of Notre Dame, Notre Dame Radiation Laboratory Shadyro, Oleg; Belarusian State University, Department of Chemistry Schiemann, Olav; University of Bonn, Institut für Physikalische und Theoretische Chemie Carmichael, Ian; University of Notre Dame, Radiation Laboratory and Department of Chemistry & Biochemistry

SCHOLARONE™
Manuscripts

ARTICLE

OH radical reactions with the hydrophilic component of sphingolipids

Alexandra Lisovskaya^{a,c*}, Oleg Shadyro^b, Olav Schiemann^c, Ian Carmichael^a

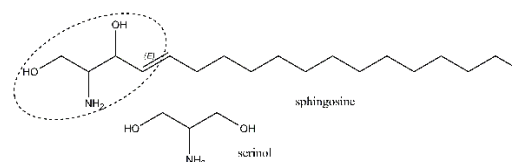
In this work, using the example of model compounds, we studied the reactions resulting from the interaction of OH radicals with the hydrophilic part of sphingolipids. We compared the stopped-flow EPR spectroscopy and pulse radiolysis with optical detection methods to characterize radical intermediates formed in the reaction of OH radicals with glycerol, serinol and N-boc-serinol. Quantum chemical calculations were also performed to help interpret the observed experimental data. It was shown that H-abstraction from the terminal carbon atom is the main process that is realized for all the studied compounds. The presence of the unsubstituted amino group ($-NH_2$) is seen to completely change the reaction properties of serinol in comparison with those observed in glycerol and N-boc serinol.

INTRODUCTION

Hydroxyl radicals are highly reactive toward many biomolecules including DNA, lipids, proteins, and carbohydrates and cause changes in their structure and functions.^{1–3} Biomolecular oxidations by OH radicals play a major role in cellular processes and can be responsible for many pathologies, including atherosclerosis, inflammatory conditions, certain cancers, and the process of aging.^{4,5}

The most frequently probed process of membrane lipid damage is peroxidation that causes oxidative damage to unsaturated fatty acid residues in the hydrophobic moiety of the membrane lipid bilayer.^{6,7} On the other hand, sphingolipids, which contain mainly saturated fatty-acid residues and modulate numerous cellular processes,^{8–10} are not subject to such oxidative events. Nevertheless, the hydrophilic head groups of sphingolipids have an aliphatic amino-alcohol core (Scheme 1) and can interact with reactive oxygen (radical) species on the surface of membranes (hydrophilic moiety). It was shown that $\cdot OH$ induces elimination of the acyl chain of sphingomyelin in its sphingosine backbone (polar part) while ceramide is stable towards such $\cdot OH$ oxidation.¹¹

Also, it was demonstrated that sphingomyelins in biological membranes act as inhibitors of lipid oxidation propagation.¹²



(1)

However, insufficient data exists on the mechanisms leading to the free radical destruction of membrane lipids that are crucial for a better understanding of the complexity of cellular processes and the origins of related pathologies (diseases).

In recent studies it was shown that the actions of gamma rays, UV-irradiation and hypochlorous acid on sphingolipids and their analogues induces damage by C-C bond cleavage in their hydrophilic moiety.^{13–16} It is believed that the mechanism includes fragmentation reactions in the hydrophilic component of these sphingolipids. These pathways differ with respect to the intermediates and products formed from those observed in peroxidation processes, and interestingly, they occur under hypoxic conditions.¹⁶

The purpose of this research is to obtain additional information on the mechanism and kinetics of the reactions of the hydrophilic component of sphingolipids with hydroxyl radicals. To do this we probed the reaction of the OH radical with small (low-weight) molecules that mimic the hydrophilic part of sphingolipids, namely 2-amino-1,3-propanediol (serinol) and its derivatives – N-boc-serinol and glycerol. Serinol is prochiral, belongs to the group of amino alcohols, and its derivatives are often used intermediates in several applications in medicine and the chemical industry.¹⁷

^a Notre Dame Radiation Laboratory, University of Notre Dame, Notre Dame, 46556 Indiana, USA

^b Department of Chemistry of the Belarusian State University, Nezavisimosti av., 4, 220030 Minsk, Belarus

^c Institute of Physical and Theoretical Chemistry, University of Bonn, Wegelerstr. 12, 53115, Bonn, Germany

*Corresponding Author: aliousk@nd.edu; orcid.org/0000-0001-7556-8977;

Electronic Supplementary Information (ESI) available: [details of any supplementary information available should be included here]. See DOI: 10.1039/x0xx00000x

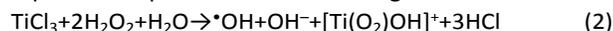
ARTICLE

Electron Paramagnetic Resonance (EPR) spectroscopy with an adjustable stopped-flow system was applied to obtain both structural and kinetic information on radical intermediates formed in the reaction of the OH radical with serinol, N-boc-serinol and glycerol to help elucidate the details of the mechanism. Quantum chemical calculations, that is Density Functional Theory with a basis set specifically designed to recover reliable isotropic hyperfine couplings, was employed to assist in the assignment of the various recorded EPR spectra. Pulse radiolysis spectrophotometric methods were used to obtain transient optical absorption spectra of the initial radicals formed from radiolysis of serinol and N-boc-serinol in aqueous solution at various pH values. Time-dependent Density Functional Theory (TD-DFT) computations of vertical excitations were performed to assist in the interpretation of the observed absorption spectra.

RESULTS

EPR spectra of radical intermediates.

Continuous flow EPR experiments together with computational chemistry have been used to study radical intermediates derived from serinol and its derivatives upon reactions with OH radicals. OH radicals were generated using a $\text{Ti}^{3+}/\text{H}_2\text{O}_2$ -Fenton system at room temperature (2). Kinetics of the species generated were measured using rapid-flow experiments with a mixing EPR resonator.



A radical at $g = 2.013$ was observed (without substrate) that corresponded to an adduct between an oxygen radical and a diamagnetic Ti^{4+} ion ($\text{Ti}^{4+}\text{-O}_2$).¹⁸ In these experiments, we used the $\text{Ti}^{3+}/\text{H}_2\text{O}_2$ -Fenton system reagent with added EDTA. EDTA complexes the metal ion and allows one to observe the reaction in neutral and alkaline solutions.^{19,20} At basic pH, the tetra-anion of EDTA is hexadentate and forms octahedral complexes with Ti^{3+} , with $g=1.954$. To separate superimposed EPR spectra of other species from those of the serinol-derived radicals in the complex mixture of the Fenton system, control experiments were performed (see Fig. S1 in Supporting Information). In the presence of a substrate, the Ti^{3+} -EDTA ligand complex appears at $g = 1.960$,^{19,20} which does not interfere with the detection of organic radicals ($g \approx 2.004$). It should be noted that we did not find the spectrum of EDTA radicals formed by the attack of the OH radical at $g = 2.0035$ (11.6 Gauss (αH), 7 Gauss (αN)), as previously reported.^{19,20} It can be assumed that their concentration was insignificant (Fig. S1).

Figure 1 shows EPR spectra of radicals formed in the reaction of 100 mM serinol with $\cdot\text{OH}$ ($\text{Ti}^{3+}/\text{H}_2\text{O}_2$ -Fenton system) at pH 3, 7 and 10.5 at room temperature recorded under fast continuous-flow conditions. We carried out experiments at different pH values since free radical fragmentation reactions are often pH sensitive. The EPR spectrum of the radicals derived from serinol in acid solutions (Fig. 1, red, pH 3) shows 12 peaks stemming from at least two distinct radicals. Upon transition to a neutral medium, this signal disappears. Increasing the pH to 10.5 the EPR signal increases again but the spectrum is different, presenting now two quartets with a total of at least 10 peaks (Fig. 1, blue).

Complementary to the experimental study, detailed quantum chemical calculations were conducted on a number of potential radicals (Figure S2). Serinol molecules tend to form intermolecular hydrogen bonds between OH and NH_2 groups resulting in 135 distinct conformational possibilities.²¹ The structures of all H-loss radicals from these conformers are obtained by DFT calculations as explained in the Methods section. Figure S3 shows optimized 3D-structures of five main conformers of neutral carbon-centered serinol radical in the first position of the carbon skeleton (C1) (aa1, ag1, ga1, ga2 and gG1).²¹ The calculated EPR parameters for all conformers of the studied compounds are given in Tables S1-S3 in Supporting Information. The optimized quantum mechanical geometries of the main radical intermediates are presented in Table S4.

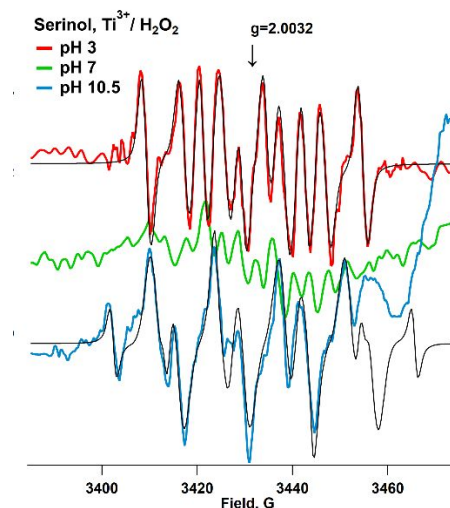


Figure 1. EPR spectra of radicals generated in the reaction of the $\text{Ti}^{3+}/\text{H}_2\text{O}_2$ -Fenton reagent with 100 mM serinol at pH 3 (red), pH 7 (green) and pH 10.5 (blue). Simulated EPR spectra of radicals are shown in black.

ARTICLE

The simulated spectra of the serinol radicals are superimposed in black on the experimental spectra in Figure 1. EPR parameters of the simulated spectra are given in Table 1.

Based on the calculated data, we predicted the formation of a carbon-centered radical cation (C1-ga2, C3-ag1) with the second component corresponding to a carbon-centered neutral radical (C1-aa1, ag1, gG1 and C3-ag1) (see Table 1, Table S1). In addition, a C1 neutral radical (ga2) also showed a contribution.

In order to study the kinetics of radical formation, EPR spectra were recorded at different reaction times from 39 ms to 0.7 ms. The signal amplitude intensity vs. mixing rates at different field values is presented in Figure 2A. Analyzing the kinetics of signals at different magnetic field values, we could see the presence of at least two radical species with different rates of formation and decay. When plotting the intensity of the radical signals against the reaction time, the resulting curve is best described by assuming an exponential decay (Fig. 2A). Based on the high rate of formation of these radicals, it can be assumed that they are formed during the first-order reaction, *i.e.*, these are the primary intermediates. This is consistent with the stimulated spectra for the carbon-centered serinol radical cation and neutral carbon-centered serinol radicals.

An EPR signal observed in the reaction of the OH radical with serinol at pH 10.5 shows 4 peaks with 13.7 G hyperfine splitting with intensity ratios 1:1:1:1 and an additional splitting (Fig. 1). The fitted spectrum contains signals from two radicals (Table 1, Table S2). The first radical can be assigned as the amino ethanol radical that can be formed as a secondary intermediate derived from a nitrogen-centered serinol radical. The additional signal can be attributed to another secondary radical intermediate.

At pH 10.5, the intensity of the EPR signal varied significantly during the time course (Fig. 2B).

It was found that these radicals are generated slowly with the maximum intensity at a reaction time of 2.5 ms and then decay very rapidly. The signal line intensity at 3411 Gauss showed a different kinetics, which may indicate the presence of another radical. Slow rates of radical formation indicate that radicals are formed in second-order reactions. This assumption is consistent with the simulated EPR spectrum (Fig. 1, Table 1).

We also collected the EPR spectra of the products formed in the reaction of OH radicals with a derivative of serinol, which has an acylated amino group – N-boc-serinol at various pH values.

Table 1. EPR parameters of the radicals derived from the reaction of studied compounds with OH radical

Radicals	Significant hyperfine coupling constants, Gauss	g value
Radicals derived from serinol at pH 3	20.8(α H), 8.9(β N), 8(β H), Line width (LW)=1.8, Line shape (LS)=0.45, Area (A)=5.9 (C1-ga2, C3-ag1 radical cations); 11.7(α H), 33(β H), LW=1.8, LS=1, A=0.8 (C1-aa1, ag1, gG1 and C3-ag1 radicals); 14(β H), 3.7(β N), LW=2.5 LS=0.18, A=6.0 (C1-ga2 radical).	2.0032 2.0032 2.0032
Radicals derived from serinol at pH 10.5	13.8 (α H), 27 (β H), 4 (β H), LW=3.06, LS=1, A=8 (amino ethanol radical); 41.5 (β H), 11 (β N), LW=1.45, LS=0.3, A=1.54 (secondary radical).	2.0021 2.0021
Radicals derived from N-boc-serinol at pH 3	17.3 (α H), 16.3 (β H), 5.9 (β N), LW=2.26, LS=0, A=18.89 (C1 radical cation); 21.9(2 β H), LW=3.56, LS=0.59, A=4.7 (C1 radical).	2.0032 2.0025
Radicals derived from glycerol at pH 1	17.3 (α H), 27.8 (2 β H), 1.2(CHO), LW=1.7, LS=0.23, A=5.4, (cis hydroxypropanal radical); 18.34(α H), 25.6(2 β H), 1.4(CHO), L=1.5, LS=0.6, A=3.8), (trans hydroxypropanal radical); 19.9 (α H), 19.4(α H), 2.25(2 γ H), LW=1.36, LS=0.4, A=1.76, (cis Hydroxyacetone radical); 19.8 (2 α H), 2.4 (2 γ H), LW=1.45, LS=0.18, A=2.1, (trans hydroxyacetone radical).	2.0045 2.0043 2.0048 2.0035
Radicals derived from glycerol at pH 11	17.346(α H), 11.05(β H), LW=1.5, LS=0.74, A=19.96 (C1 glycerol radical); 10.0(4 β H), LW=1.1, LS=0.6, A=6.3 (C2 glycerol radical).	2.0031 2.0029

Figure 3 shows EPR spectra of transient radicals formed from N-boc-serinol upon reaction with the $\text{Ti}^{3+}/\text{H}_2\text{O}_2$ - Fenton system at pH 3, 7 and 11.

In alkaline as well as in neutral solutions of N-boc-serinol, the signal is practically unnoticeable (Fig. 3).

The spectrum of the radical(s) derived from N-boc-serinol in acid solutions differs from that observed for serinol.

The simulated EPR spectra of possible N-boc-serinol radicals showed that the experimental spectrum in acid solution corresponds to a combination of two radicals.

ARTICLE

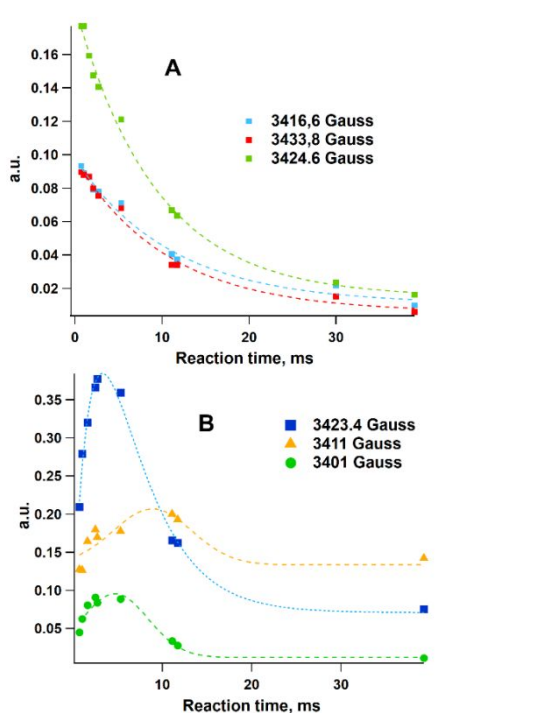


Figure 2. Reaction kinetics for serinol with OH radical at different pH values. The EPR signal intensity for radicals generated in the reaction of Ti^{3+}/H_2O_2 -Fenton with 100 mM serinol at pH 3 (the signal line amplitude) vs. reaction time fitted to the exponential decay (A) and with 50 mM serinol at pH 10.5 (the signal line amplitude) vs reaction time (B).

The simulated EPR spectra of radicals formed in the reaction of OH radical with N-boc-serinol at pH 3 are shown in black in Figure 3. The signal corresponds to a superposition of the C1 radical cation with the C1 radical (Table 1, Table S2).

The kinetics of the reaction of N-boc-serinol with the OH radical in acid solutions showed the same behavior as for serinol, which suggests the formation of primary radical intermediates.

To establish the effect of the amino group on the structure of radicals derived from serinol, we also probed glycerol solutions at different pH values.

Figure 4 shows the EPR spectra of transient radicals formed from glycerol upon reaction with the Ti^{3+}/H_2O_2 -Fenton system at pH 1, 7 and 11 at a reaction time of 2.5 ms. The signals of glycerol radicals are significantly different from either serinol or N-boc-serinol. The signal from glycerol radical intermediates is much more intense in alkaline solutions and has fast formation rate and an exponential decay similar to that seen in Figure 2(A).

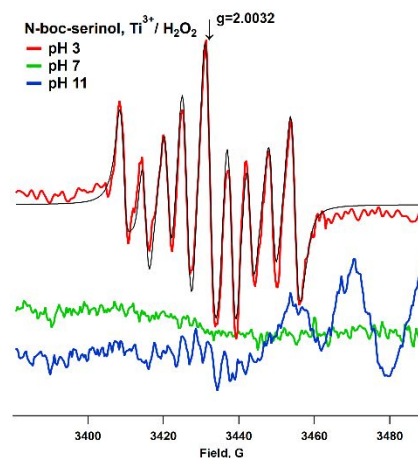


Figure 3. EPR spectra of radicals generated in the reaction of the Ti^{3+}/H_2O_2 -Fenton with N-boc-serinol at pH 3, pH 7 and pH 11 recorded at a reaction time of 2.5 ms. Simulated EPR spectra of radicals are shown in black.

The fitted EPR parameters for radicals derived from glycerol are given in Table 1. The EPR signal in alkaline solutions corresponds to the C1* glycerol radical with hfcs from 2 hydrogens (Table 1).

The simulated spectra of the C1* glycerol radicals are superimposed in black on the experimental spectrum in Figure 4. The contribution of an additional signal from the C2* glycerol radical ($4H\beta$) is also visible (10%). The structure of the spectrum obtained in acidic glycerol solutions (Fig. 4) shows 7 main peaks that include signals from the hydroxypropanal radical ($hc2^*$), ~70%, with hfcs corresponding to both its *cis*- and *trans*- forms.

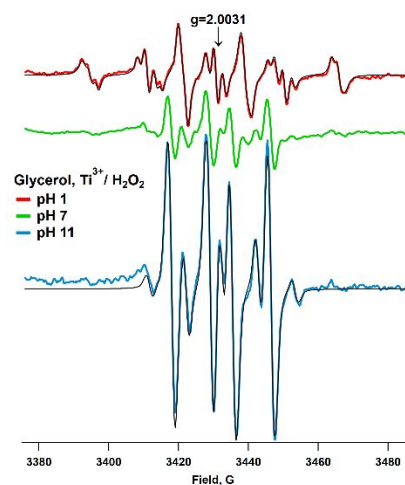


Figure 4. EPR spectra of radicals generated in the reaction of the Ti^{3+}/H_2O_2 -Fenton system with glycerol at pH 1 (red), pH 7 (green) and pH 11 (blue). Simulated EPR spectra of radicals are shown in black.

ARTICLE

About 30 % of the signal is the contribution from the hydroxyacetone radical (hC1^*) also with hfc's of its *cis*- and *trans*- forms.

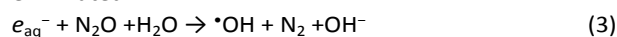
Previously it was found that EPR spectra observed in the UV-induced reaction of glycerol with H_2O_2 in acid solutions were composed of radicals hC2^* and hC1^* produced by acid-catalyzed elimination of water from C1^* and C2^* glycerol radicals²². The data obtained in this work match the EPR parameters obtained previously (Table S3)^{22,23}.

The signal intensity was the highest at a reaction time of 2.5 ms, as shown for serinol radicals formed in alkaline solutions, implying that these radicals were generated in second-order reactions.

At neutral pH, the signal is much weaker and the structure of glycerol radicals is similar to that observed in an alkaline medium with additional splittings from hC1^* and hC1^* radicals (Fig. 4). Presumably, the C1^* glycerol radical begins to undergo acid-catalyzed dehydration upon transition to pH neutrality.

Transient absorption spectra of radical intermediates. Pulse radiolysis.

The OH-induced free radical reactions of serinol and N-boc-serinol were also examined at various pH values using pulse radiolysis. Figure 5(A) shows the transient absorption spectra measured after pulse radiolysis of solutions containing 10 mM serinol saturated with N_2O to scavenge e_{aq}^- (3-4). In the presence of N_2O ($2.8 \times 10^{-2} \text{ mol dm}^{-3}$) the reaction of serinol with the hydrated electron is completely eliminated.



An absorption spectrum with a maximum at about 300 nm formed within 200 μs after the pulse in both neutral and

alkaline solution (Fig. 5(A)). With an increase in pH up to pH 12, the intensity at 300 nm decreases and a shoulder grows in at 350-360 nm. In acidic solutions with pH 4, the signal at 300 nm disappears.

Figure 5(B) shows the kinetics of transients formed in 10mM serinol solutions at 303 nm at pH 7 and 10.5 200 μs after the pulse. The fit curves are shown in black. The rate constants of the $\cdot\text{OH}$ reaction with serinol for their formation have been measured at various concentrations of serinol and different doses at 303 nm at pH 7 and 10.5.

The pseudo-first-order rate constants of the formation of the serinol radical at 303 nm were plotted as a function of substrate concentration (Fig. 6). They have a linear character with the slope representing the second-order rate constant for the formation of radicals from reaction of serinol with the OH radical equal to $1.56 \pm 0.3 \times 10^{10} \text{ M}^{-1}\text{s}^{-1}$ at pH 7 and $4.02 \pm 0.5 \times 10^{11}$ at pH 10.5. It can be seen that the rate of formation of serinol transients is about 20 times faster in an alkaline medium. At the same time, the signal is more intense in neutral solutions.

To assist with the interpretation of our experiments, we calculated transient absorption spectra of possible radicals formed during reaction of the OH radical with serinol and N-boc-serinol in aqueous solutions at different pH (Fig. S2). First, we used the time-dependent DFT (TD-DFT) method with the B3LYP functional and a flexible augmented and polarized triple-zeta basis set.

Tables S1-S2 presents data on the calculated vertical excitation energies of the radicals derived in the reaction of serinol and N-boc-serinol with OH radical. Table 2 shows the comparison of significant experimental data and suitable calculated excitation energies of the radicals formed in the reaction of serinol and N-boc-serinol with the OH radical.

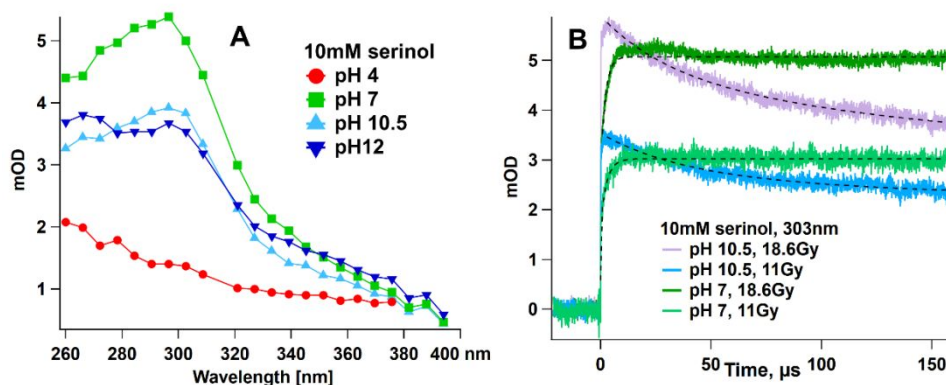


Figure 5. (A) Transient absorption spectra observed 200 μs after 5 ns pulse radiolysis ($\sim 16.3 \text{ Gy}$) in N_2O -saturated aqueous solution containing 10 mM serinol at pH 4 (\bullet), pH 7 (\blacksquare), pH 10.5 (\blacktriangle) and pH 12 (\blacktriangledown). (B) Kinetics of transients formed 200 μs after 5 ns pulse radiolysis at 303 nm in 10 mM serinol solutions at pH 7 and 10.5, saturated with N_2O .

ARTICLE

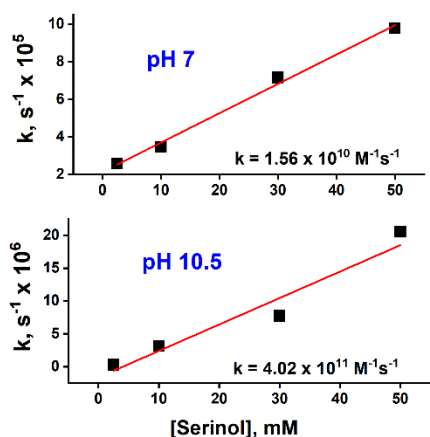


Figure 6. Plots of the observed pseudo-first-order rate constants of the radical formation of at 303 nm as a function of serinol concentration at pH 7 and 10.5 in N_2O -saturated aqueous solution.

Based on the calculated spectra, the signal of serinol transients in acidic solutions may correspond to a superposition of aa1 and ga1 conformers of C1 serinol radical cations (Table 2). The TD-DFT calculated spectrum of serinol carbon-centered radical cations showed low intensity signals, and an additional shoulder appears at 320 nm (Table S1).

In neutral serinol solutions, the absorption maximum at 300 nm can be attributed to the neutral carbon-centered serinol radicals (C1-aa1,ag1, C3-ga1,ga2). The suitable calculated spectra (artificially broadened by assuming a 0.333 eV half-width) are superimposed on the experimental one with a relative intensity and width in the Figure S4.

In alkaline solutions, the spectral maximum of serinol transients is shifted to the red with an additional shoulder at 330-390 nm.

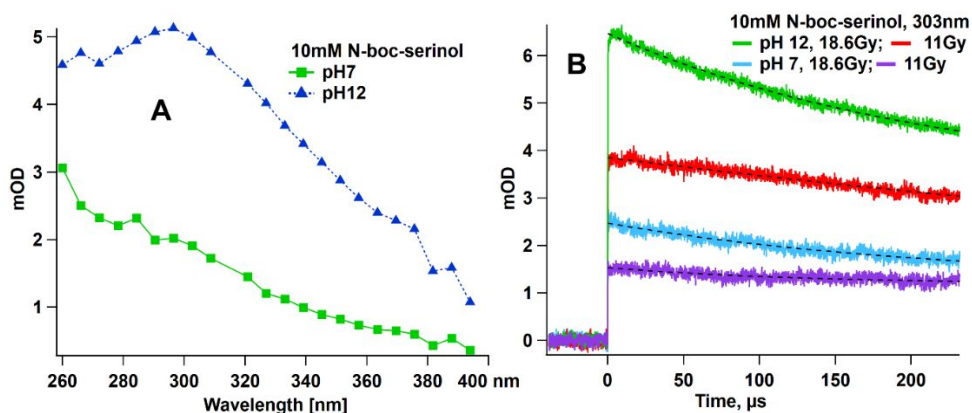


Figure 7 (A) Transient absorption spectra observed in 200 μs after 5 ns pulse radiolysis (~ 16.3 Gy) in N_2O -saturated aqueous solution containing 10 mM N-boc-serinol at pH 7 (■) and pH 12 (▲). (B) Kinetics of transients within 200 μs after 5 ns pulse radiolysis at 303 nm in 10 mM N-boc-serinol solutions at pH 7 and 12, saturated with N_2O .

Table 2. Significant excitation energies of the radicals formed in the reaction of serinol and N-boc-serinol with OH radical

Radicals	Experimental excitation energies, nm	Calculated excitation energies (oscillator strengths), nm
Radicals derived from serinol at pH 3	266(0.002), 278(0.0018), 302(0.0013), 333(0.001)	269(0.02), 322(0.01) (C1 radical cation - aa1, ga1).
Radicals derived from serinol at pH 7	296(0.054)	293.5(0.033) (C1 radical - aa1, ag1); 298(0.02) (C3 radical - ga1, ga2).
Radicals derived from serinol at 10.5	266(0.003), 296(0.0039), 345(0.0013), 387(0.007)	307(0.025), 350(0.016), 403(0.025) (C2 radical - ga1, ga2); 250(0.01), 356(0.004) N-centered radical (averaged).
Radicals derived from N-boc-serinol at pH 7	260(0.003), 296(0.002), 320(0.015)	290(0.02), 337(0.003) (C1 radical).
Radicals derived from N-boc-serinol at pH 11	296(0.005), 327(0.004), 376(0.002)	284(0.06), 309(0.02), 343(0.02) (C2 radical); 290(0.02), 337(0.003) (C1 radical).

The calculated spectrum from the neutral C2 serinol radical has an intense broad signal at 310-400 nm.

The calculated optical spectrum of the nitrogen-centered serinol radical showed weak absorption at 320-340 nm with an additional shoulder at 515 nm (Table S1), which is not observed in the experimental data.

ARTICLE

Therefore, it can be assumed that a superposition of various serinol radicals occurs in alkaline solutions (see Table 2).

Figure 7A shows the transient absorption spectra observed 200 μ s after a 5 ns electron pulse in N_2O -saturated aqueous solution containing 10 mM N-boc-serinol at pH 7 (■) and pH 12 (▲). In this case, in acid solutions, the absorption signal was in the ultraviolet region, less than 230 nm. In a neutral medium, the spectrum looks like that in serinol solutions at pH 3. Upon transition to an alkaline medium, broad intense signals appear at 290 nm with a shoulder at 320–380 nm. It follows from this that completely different processes occur during the interaction of OH radicals with these substrates at alkaline pH.

The kinetics of transients formed in 10 mM N-boc-serinol solutions at 303 nm at pH 7 and 12 within 200 μ s after pulse radiolysis is presented in Figure 7B. As can be seen from these kinetics, N-boc-serinol transients are rapidly formed and then decompose by analogy with serinol transients at pH 10.5.

The TD-DFT calculated and experimental excitation energies of N-boc-serinol radicals are presented in Table 2. As can be seen from these data, the calculated spectra of neutral C1 carbon-centered radical correspond to the experimental spectrum at pH 7 (Table 2, Table S2). The absorption spectrum of N-boc-serinol transients produced in reaction with $\cdot OH$ at pH 12 has a broad band from 280 to 350 nm. The observed spectrum of N-boc-serinol transients in alkaline solutions can be attributed to a combination of neutral carbon-centered radicals in the first and second position of the carbon skeleton (C1, C2).

DISCUSSION

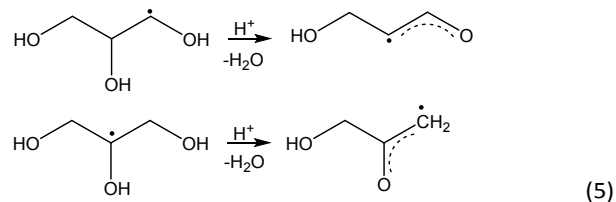
In this work we applied pulsed radiolysis and stopped-flow EPR spectroscopy to obtain information on the structure of radical intermediates and their kinetics formed in the reactions of $\cdot OH$ with a structural analogue to the hydrophilic part of sphingolipids. We used the concept of homology in structure when we selected low molecular weight lipid analogues – serinol and N-boc serinol. To evaluate the contribution of the amino group, we studied the radical intermediates that are formed in the reaction of glycerol with the OH radical. Glycerol is a structural analogue of hydroxyl-containing phospholipids, which are also prone to fragmentation reactions in their hydrophilic part.^{24–26} In addition, a recent review examined in detail the reactions of reactive oxygen species with lipids, which proceed without oxygen.¹⁶

Previously, OH-induced reactions of amino alcohols and other amino acids were studied using steady-state radiolysis of their aqueous solutions.^{27–29} Radiolysis product analysis can give information on products eventually formed but does not provide direct evidence of the primary steps that occur in radical reactions. The purpose of this work was to identify such prompt radical intermediates derived from serinol and its derivatives in reaction with $\cdot OH$ and to probe their kinetics, which have not been previously reported.

It is well known that the interaction of OH radicals with alcohols will mainly lead to the formation of carbon-centered radicals from the starting molecules by H-atom abstraction. Further transformations of the C-centered radicals initially formed depend on their structures (functional groups) and on the environment.^{22,23,30,31–33}

The data obtained in this work on EPR spectra of glycerol in acid solutions confirm the presence of both the 3-hydroxypropanal radical and the hydroxyacetone radical, which were formed upon acid-catalyzed dehydration of the C1 and C2 glycerol radicals according to Scheme (5). Similar reactions have been observed for glycerol,²² glycerol-1-phosphate,^{23,34} ethylene glycol^{31–33} and hydrated glycolaldehyde³⁵ by pulse radiolysis and EPR spectroscopy. It was shown that elimination of water from C1 and C2 glycerol radicals is the dominant process in acidic solutions.^{22,23} The suggested dehydration reaction mechanism was proposed to go through a six-membered transition state.

It seems that the probability of the fragmentation of C1 and C2 glycerol radicals is greatly reduced in neutral solutions. Moreover, the EPR spectra of radicals formed in glycerol solutions at pH 7 and 11 mainly correspond to the C1 glycerol radical with an additional contribution from C2 (Table 1).

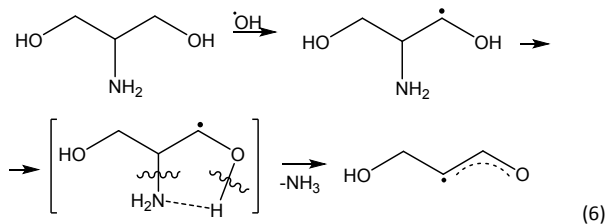


Serinol exist in a protonated form at pH values less than 5, since the pK_b of serinol is 5.45. The primary stage of the reaction of serinol with the OH radical, which was recorded by pulsed radiolysis and EPR, involves the formation of the C1 radical cation and C1 neutral radical. In contrast to our observations for glycerol, in serinol solutions we could not

ARTICLE

identify 3-hydroxypropanal and hydroxyacetone radicals formed during rapid acid-catalysed deamination. Thus, the protonation of the amino group blocks that fragmentation process of C1 serinol radicals in acid solutions.

Based on quantum chemical calculations, we have determined the relative energies of the various radicals formed upon H abstraction from our starting compounds. In each case, radicals formed at C2 were shown to be the more stable (Table S1). The fact that the observed EPR spectra indicate the presence of radicals at C1 and/or C3 implies that the formation process is under kinetic control. Similar preference for the formation of C1 radicals was obtained previously for glycerol radicals, both in this work and previously.^{22,23,35} It can be assumed that the deamination process of serinol is more energetically favorable than dehydration and is stabilized by the formation of a transition state with hydrogen bonds. As previously mentioned, serinol molecules form intermolecular hydrogen bonds between OH and NH₂ groups.²¹ The most abundant conformer ga1 exhibits a chain of O–HN and N–HO hydrogen bonds, where the amino group simultaneously acts as both a proton donor and an acceptor. Previously, it was found that C1 carbon-centered serinol radicals in neutral solutions decay through further deamination with accumulation of the final product 3-hydroxypropanal, which is the main product in neutral solutions.^{27–29} The mechanisms of [•]OH-induced serinol fragmentation reactions in neutral solutions includes the formation a five membered transition state of the C1 radical, due to hydrogen bonding, followed by breaking of the 2β bonds (in relation to the radical center), as shown in scheme (6).

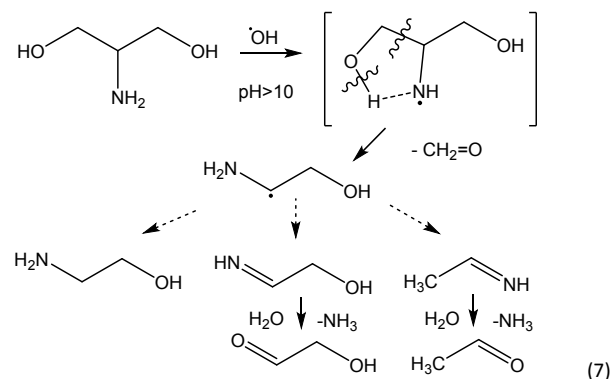


Similar to serinol, [•]OH-induced processes were obtained for N-boc-serinol in acidic and neutral solutions. It was previously shown that ethanolamine and serine phosphates in neutral solutions form mainly C1 radicals at the α-position to the phosphate and phosphate elimination from these radicals does not take place when the amino group is protonated.²³

From the calculated data on optical absorption we can propose the formation of C1(3) serinol radicals (averaged transients from conformers) at pH 7 (Table 2).

The data obtained showed that transients formed in the reactions of the compounds under study with the OH radical in alkaline solutions were completely different. In the case of glycerol, the primary C1 radical is the main intermediate in alkaline media. The presence of an amino group in the structure of serinol completely changes the reaction properties of the molecule. In neutral and alkaline solutions the amino group of serinol is in the unprotonated state (pK_a = 12.2). Under these conditions, the process of C2 radical formation becomes energetically more favorable. From the optical absorption of the intermediates, it can be seen that C2 serinol radicals have a very short lifetime. Therefore, it was not possible to observe them by our stopped-flow EPR method. Similar processes for the formation of the C2 radical were also demonstrated for N-boc-serinol at pH 11.

Nevertheless, it was previously found that during radiolysis of solutions of amino alcohols, along with the deamination process, destruction products of the carbon skeleton were formed.^{27–29} The yields of fragmentation products were higher in alkaline solutions. Consequently, in the case of serinol, the formation of nitrogen-centered radicals is also realized. It was proposed that the interaction of electrophilic OH radicals with amino group leads to the formation of aminyl radicals, which further fragment through a five-membered transition state (Scheme 7).



The radicals detected from serinol in alkaline solutions by the EPR method are secondary intermediates that have a signal structurally similar to that of the aminoethanol radical with the addition of other hyperfine splittings. The optical absorption spectrum of nitrogen-centred radical is most likely not intense and could not be distinguished. The replacement of the hydrogen atom in the amino group of

ARTICLE

the N-boc-serinol molecule leads to blocking of this process. No EPR signal was observed in alkaline solutions of N-boc-serinol, which may indicate the participation of the amino group in the formation of this serinol intermediate.

CONCLUSION

In this work, a comparison of radical intermediates of radicals formed during the reaction of OH radicals with glycerol, serinol and N-boc-serinol was carried out using stopped-flow EPR spectroscopy and pulse radiolysis. Based on both obtained experimental results and calculated data, the reaction mechanisms of the studied compounds were proposed. It has been shown that in a neutral medium, all the compounds undergo H-abstraction mainly from the first atom of the carbon chain in reactions with an OH radical, though energetically less favorable than abstraction at C2, based on computational chemistry data. These facts should be taken into account when considering the processes of sphingolipid destruction in neutral solutions. In acidic solutions, glycerol radicals undergo fast acid-catalyzed dehydration. This process is not realized for serinol or N-boc-serinol molecules, since, in an acidic medium, the amino group is protonated, thus preventing rapid implementation by such secondary reactions (deamination and dehydration).

The presence of an amino group completely changes the reaction properties of serinol in alkaline solutions and leads to the occurrence of dehydration and destruction processes. The stopped-flow EPR method made it possible to identify and describe the radicals derived from the studied compounds, the formation rate of which do not exceed $1 \times 10^{10} \text{ M}^{-1} \text{ s}^{-1}$. For example, we identified the formation of short-lived serinol and N-boc-serinol radicals in an alkaline medium by the method of pulse radiolysis, though they are not detected by the stopped-flow EPR. At the same time, for acidic solutions of glycerol and alkaline solutions of serinol, we have shown the possibility of catching radical intermediates formed in secondary reactions on the basis of the kinetics of the EPR signal.

Thus, in this work we present a comparison of two methods that make it possible to obtain information about the structure and also the kinetics of the formed radical intermediates. Of course, the EPR method is much more useful in determining the structure of radicals. While the pulse radiolysis method makes it possible to record the absorption spectrum and kinetics of short-lived radicals,

which cannot be detected by the stopped-flow EPR method.

METHODS

Pulse radiolysis experiments. All chemicals were commercial samples of high purity and used without further purification. The pulse radiolysis experiments were performed using an 8 MeV Linear Accelerator (LINAC) at the Notre Dame Radiation Laboratory with pulses of 2 ns duration. A multichannel detection system with a 1000 W xenon lamp was used for the UV-visible transient absorption measurements at short times. A multichannel system recorded an array of 24 monochromatic kinetic signals on all input channels of 6 synchronously triggered Tektronix oscilloscopes as described earlier.³⁶ For pulse radiolysis dosimetry, 10 mM KSCN solutions saturated with N₂O were used. The radiation chemical yield of (SCN)₂[•] was taken as $(5.2 \pm 0.05) \times 10^{-4} \text{ m}^2 \text{ J}^{-1}$ with $\epsilon = 7580 \text{ M}^{-1} \text{ cm}^{-1}$.³⁷

Stopped flow EPR spectroscopy. CW-EPR experiments were carried out in a Ti³⁺/EDTA/H₂O₂-Fenton system with a Bruker ER 4117 MX Dielectric Mixing Resonator installed on a Bruker EMX Micro EPR spectrometer. For each experiment, the solutions were prepared freshly in argon saturated ultrapure water and stored under an argon atmosphere. For the Fenton-like reaction, 100 mL of each of the two reactant solutions were prepared. Solution 1 consisted of TiCl₃ (8.8 mM), H₂O₂ (160 mM), together with H₂SO₄ (180 mM) or EDTA (14 mM). pH control was achieved using 2.5 M NaOH. Solution 2 containing 50-100 mM of substrate at different pH values. The flow rates were determined by measuring the emptying times of the syringes, and the reaction times were calculated taking into account the geometry of the resonator as was shown in previously.³⁸ To determine the mixing capabilities of the BRUKER ER 4117 MX resonator, the literature-known reaction between TEMPO (2,2,6,6-Tetramethylpiperidinyloxy) and sodium dithionite was checked at different concentration ratios.

Simulations of EPR spectra were carried out using the SpinFit module in the Bruker Xenon software.

Theoretical calculations. The theoretical calculations were performed using the Gaussian 16, Rev. B.01 program package.³⁹ For serinol, radical structures were derived from those of a set of neutral molecular conformers kindly provided by Dr. M.E. Sanz, Kings College, London, by simply removing the appropriate hydrogens before reoptimization. Similar starting structures for glycerol were

ARTICLE

provided by Prof. R. Chelli (University of Florence). Optimized geometries of the resulting radical species were obtained using the B3LYP functional⁴⁰ with a flexible aug-cc-pVTZ basis set.⁴¹ The effect of the solvent was modeled by embedding the radicals in a self-consistent reaction field as implemented in the integral equation formalism of the polarized cavity model,⁴² with parameters appropriate for water. Isotropic hyperfine coupling constants were first obtained by single point calculations using the same functional with a basis set specifically designed for satisfactory recovery of the Fermi contact spin density⁴³ and the same solvent model. Finite temperature corrections were made via inclusion of the effects of anharmonic vibrations.⁴⁴

Electronic transition energies and oscillator strengths were calculated by the TD-DFT approach⁴⁵ at the optimized geometries initially using the B3LYP functional (again with the aug-cc-pVTZ basis set) but eventually employing a range-separated hybrid functional (ω B97xD).⁴⁶ The latter functional provides a more reliable description of any charge-transfer component in the observed electronic transitions.

Conflicts of interest

There are no conflicts to declare.

ACKNOWLEDGMENTS

The pulse radiolysis experiments and theoretical calculations at the Notre Dame Radiation Laboratory are supported by the U.S. Department of Energy, Office of Science, Office of Basic Energy Sciences under award number DE-FC02-04ER15533. EPR spectroscopy work at the Institute of Physical and Theoretical Chemistry, University of Bonn was supported by the German Academic Exchange Service (DAAD-Research grant, 57314022). This is document number NDRL-5298 from the Notre Dame Radiation Laboratory.

REFERENCES

- 1 M. J. Davies, Protein oxidation and peroxidation, *Biochem. J.*, 2016, **473**, 805–825.
- 2 P. O'Neill and E. M. Fielden, *Primary Free Radical Processes in DNA*, 1993.
- 3 E. Niki, Lipid peroxidation: Physiological levels and dual biological effects, *Free Radic. Biol. Med.*, 2009, **47**, 469–484.
- 4 B. Halliwell and J. M. C. Gutteridge, *Free Radicals in Biology and Medicine*, Oxford University Press, 2015.
- 5 H. Sies, Oxidative stress: a concept in redox biology and medicine, *Redox Biol.*, 2015, **4**, 180–183.
- 6 N. A. Porter and C. R. Wagner, Phospholipid autoxidation, *Adv. Free Radic. Biol. Med.*, 1986, **2**, 283–323.
- 7 V. E. Kagan, *Lipid Peroxidation In Biomembranes*, CRC Press, 2018.
- 8 Y. A. Hannun and L. M. Obeid, Sphingolipids and their metabolism in physiology and disease, *Nat. Rev. Mol. Cell Biol.*, 2018, **19**, 175–191.
- 9 M. Maceyka and S. Spiegel, Sphingolipid metabolites in inflammatory disease, *Nature*, 2014, **510**, 58–67.
- 10 M. L. Kraft, *Front. Cell Dev. Biol.*, 2017, **4**.
- 11 T. Melo, E. Maciel, M. M. Oliveira, P. Domingues and M. R. M. Domingues, Study of sphingolipids oxidation by ESI tandem MS, *Eur. J. Lipid Sci. Technol.*, 2012, **114**, 726–732.
- 12 G. Coliva, M. Lange, S. Colombo, J. P. Chervet, M. Rosario Domingues and M. Fedorova, Sphingomyelins prevent propagation of lipid peroxidation—LC-MS/MS evaluation of inhibition mechanisms, *Molecules*, , DOI:2020.
- 13 A. G. Lisovskaya, I. P. Edimecheva and O. I. Shadyro, in *Photochemistry and Photobiology*, 2012, vol. 88, pp. 899–903.
- 14 O. Shadyro, A. Lisovskaya, G. Semenkova, I. Edimecheva and N. Amaegberi, Free-radical destruction of sphingolipids resulting in 2-hexadecenal formation, *Lipid Insights*, 2015, **8**, 1–9.
- 15 A. G. Lisovskaya, K. O. Prochenko and O. I. Shadyro, Photochemical transformations of sphingosine and serinol in aqueous and ethanol solutions, *High Energy Chem.*, 2017, **51**, 321–326.
- 16 O. Shadyro and A. Lisovskaya, ROS-induced lipid transformations without oxygen participation, *Chem. Phys. Lipids*, 2019, **221**, 176–183.
- 17 B. Andreeßen and A. Steinbüchel, Serinol: Small molecule - big impact, *AMB Express*, 2011, **1**, 1–6.
- 18 M. Kobayashi, V. Petrykin, K. Tomita and M. Kakahana, New water-soluble complexes of titanium with amino acids and their application for synthesis of TiO₂ nanoparticles, *J. Ceram. Soc. Japan*, 2008, **116**, 578–583.
- 19 G. Lassmann, L. A. Eriksson, F. Lenzian and W. Lubitz, Structure of a Transient Neutral Histidine Radical in Solution: EPR Continuous-Flow Studies in a

ARTICLE

- Ti³⁺/EDTA–Fenton System and Density Functional Calculations, *J. Phys. Chem. A*, 2000, **104**, 9144–9152.
- 20 H. Paul and H. Fischer, Elektronenspinresonanz kurzlebiger Radikale aus einigen Aminosäuren und Amiden, *Ber.Bunsenges.Phys.Chem.*, 1969, **73**, 972–980.
- 21 D. Loru, I. Peña, J. L. Alonso and M. Eugenia Sanz, Intramolecular interactions in the polar headgroup of sphingosine: Serinol, *Chem. Commun.*, 2016, **52**, 3615–3618.
- 22 S. Steenken, G. Behrens and D. Schulte-Frohlinde, Radiation Chemistry of DNA Model Compounds. Part IV. Phosphate Ester Cleavage in Radicals Derived from Glycerol Phosphates, *Int. J. Radiat. Biol. Relat. Stud. Physics, Chem. Med.*, 1974, **25**, 205–209.
- 23 A. Samuni and P. Neta, Hydroxyl radical reaction with phosphate esters and the mechanism of phosphate cleavage, *J. Phys. Chem.*, 1973, **77**, 2425–2429.
- 24 O. Shadyro, I. Yurkova, M. Kisel, O. Brede and J. Arnhold, Formation of phosphatidic acid, ceramide, and diglyceride on radiolysis of lipids: Identification by MALDI-TOF mass spectrometry, *Free Radic. Biol. Med.*, 2004, **36**, 1612–1624.
- 25 I. Yurkova, M. Kisel, J. Arnhold and O. Shadyro, Iron-mediated free-radical formation of signaling lipids in a model system, *Chem. Phys. Lipids*, 2005, **137**, 29–37.
- 26 O. Shadyro, S. Samovich and I. Edimecheva, *Free Radic. Biol. Med.*, 2019, **144**, 6–15.
- 27 A. G. Lisovskaya, O. I. Shadyro and I. P. Edimecheva, A new mechanism for photo- and radiation-induced decomposition of sphingolipids, *Lipids*, 2011, **46**, 271–276.
- 28 A. G. Lisovskaya, A. A. Sladkova, A. A. Sosnovskaya and O. I. Shadyro, Reactions of aminyl radicals during radiolysis and photolysis of aqueous solutions of amino alcohols and their derivatives, *High Energy Chem.*, 2012, **46**, 241–246.
- 29 A. A. Sladkova, A. G. Lisovskaya, A. A. Sosnovskaya, I. P. Edimecheva and O. I. Shadyro, Destruction of amino alcohols and their derivatives on radiolysis and photolysis in aqueous solutions, *Radiat. Phys. Chem.*, 2014, **96**, 229–237.
- 30 G. Koltzenburg, T. Matsushige and D. Schulte-Frohlinde, The Mechanism of Decay of the Radical HO—CH—CH₂—OCOCH₃ in Aqueous Solutions. A Conductometric Pulse Radiolysis Study, *Zeitschrift für Naturforsch. B*, 1976, **31**, 960–964.
- 31 R. Livingston and H. Zeldes, Paramagnetic Resonance Study of Liquids during Photolysis. III. Aqueous Solutions of Alcohols with Hydrogen Peroxide¹, *J. Am. Chem. Soc.*, 1966, **88**, 4333–4336.
- 32 R. Livingston and H. Zeldes, Paramagnetic resonance study of liquids during photolysis: Hydrogen peroxide and alcohols, *J. Chem. Phys.*, 1966, **44**, 1245–1259.
- 33 B. C. Gilbert, J. P. Larkin and R. O. C. Norman, Electron spin resonance studies. Part XXXIII. Evidence for heterolytic and homolytic transformations of radicals from 1,2-diols and related compounds, *J. Chem. Soc. Perkin Trans. 2*, 1972, 794–802.
- 34 M. Fitchett, B. C. Gilbert and R. L. Willson, Fragmentation reactions of radicals formed from sugar phosphates and the hydroxyl radical: An investigation by electron spin resonance spectroscopy and pulse radiolysis, *J. Chem. Soc. Perkin Trans. 2*, 1988, 673–689.
- 35 S. Steenken, W. Jaenicke-Zauner and D. Schulte-Frohlinde, Photofragmentation of hydroxyacetone, 1,3-dihydroxyacetone, and 1,3-dicarboxyacetone in aqueous solution. An EPR study, *Photochem. Photobiol.*, 1975, **21**, 21–26.
- 36 A. Lisovskaya, K. Kanjana and D. M. Bartels, One-electron redox kinetics of aqueous transition metal couples Zn^{2+/⁺}, Co^{2+/⁺}, and Ni^{2+/⁺} using pulse radiolysis, *Phys. Chem. Chem. Phys.*, 2020, **22**, 19046–19058.
- 37 G. V. Buxton and C. R. Stuart, Re-evaluation of the thiocyanate dosimeter for pulse radiolysis, *J. Chem. Soc. Faraday Trans.*, 1995, **91**, 279.
- 38 E. Schubert, T. Hett, O. Schiemann and Y. Nejatjahromy, EPR studies on the kinetics of the α -hydroxyethyl radical generated by Fenton-like chemistry, *J. Magn. Reson.*, 2016, **265**, 10–15.
- 39 M. J. Frisch, G. W. Trucks, H. E. Schlegel, G. E. Scuseria, M. A. Robb, J. R. Cheeseman, G. Scalmani, V. Barone, G. A. Petersson, F. O., J. B. Foresman and J. D. Fox, *Gaussian, Inc., Wallingford CT*, 2016.
- 40 A. D. Becke, Density-functional thermochemistry. III. The role of exact exchange, *J. Chem. Phys.*, 1993, **98**, 5648–5652.
- 41 T. H. Dunning, Gaussian basis sets for use in correlated molecular calculations. I. The atoms boron through neon and hydrogen, *J. Chem. Phys.*, 1989, **90**, 1007–1023.
- 42 E. Cancès, B. Mennucci and J. Tomasi, A new integral equation formalism for the polarizable continuum model: Theoretical background and applications to isotropic and anisotropic dielectrics, *J. Chem. Phys.*, 1997, **107**, 3032–3041.
- 43 R. Stenutz, I. Carmichael, G. Widmalm and A. S. Serianni, Hydroxymethyl Group Conformation in

ARTICLE

- Saccharides: Structural Dependencies of $2 J_{HH}$, $3 J_{HH}$, and $1 J_{CH}$ Spin-Spin Coupling Constants, *J. Org. Chem.*, 2002, **67**, 949–958.
- 44 J. Bloino and V. Barone, *J. Chem. Phys.*, 2012, 136.
- 45 R. E. Stratmann, G. E. Scuseria and M. J. Frisch, An efficient implementation of time-dependent density-functional theory for the calculation of excitation energies of large molecules, *J. Chem. Phys.*, 1998, **109**, 8218–8224.
- 46 J. Da Chai and M. Head-Gordon, Long-range corrected hybrid density functionals with damped atom-atom dispersion corrections, *Phys. Chem. Chem. Phys.*, 2008, **10**, 6615–6620.

